Effect of H_2S and HCl on solid oxide fuel cells fed with simulated biosyngas containing primary tar

Cavalli, Alessandro; Bernardini, Roberta; Del Carlo, Tommaso; Aravind, Purushothaman Vellayani

DOI
10.1002/ese3.434

Publication date
2019

Document Version
Final published version

Published in
Energy Science and Engineering

Received: 8 May 2019 | Revised: 4 July 2019 | Accepted: 18 July 2019

DOI: 10.1002/ese3.434

RESEARCH ARTICLE

Energy Science & Engineering Open Access

Effect of H_2S and HCl on solid oxide fuel cells fed with simulated biosyngas containing primary tar

Alessandro Cavalli[1] | **Roberta Bernardini**[2] | **Tommaso Del Carlo**[2] | **Purushothaman Vellayani Aravind**[1]

[1]Process & Energy Department, 3me Faculty, Delft University of Technology, Delft, The Netherlands

[2]Department of Energy, Systems, Territory and Construction Engineering, Faculty of Engineering, University of Pisa, Pisa, Italy

Correspondence
Alessandro Cavalli, Process & Energy Department, 3me Faculty, Delft University of Technology, Leeghwaterstraat 39, 2628 CB Delft, The Netherlands.
Email: a.cavalli@tudelft.nl

Funding information
European Union's Horizon 2020 Research and Innovation Program, Grant/Award Number: 641229

Abstract

Integrated biomass gasifier solid oxide fuel cell systems are an alternative to fossil-fuel-based combined heat and power generators. However, biosyngas contaminants represent a bottleneck for small-scale systems. In this work, we present the results of experiments on the effects of H_2S, HCl, and acetic acid as model primary tar on Ni-GDC SOFC. First, the effects of 17-128 g/Nm^3 dry basis acetic acid were studied. On a second cell, 0.8 and 1.3 ppm(v) H_2S were added to the simulated biosyngas anode flow. After a full recovery, the cell was exposed to 42 g/Nm^3 acetic acid and 0.8 ppm(v) H_2S. On a third cell, 3.4, 20, and 50 ppm(v) HCl were tested and, after a recovery period, 42 g/Nm^3 acetic acid and HCl were added. Even 0.8 ppm(v) H_2S caused an immediate voltage drop. H_2S affected CH_4 reforming and water-gas shift reaction. Differently, even 50 ppm(v) HCl appeared not to significantly affect these reactions. Acetic acid increased the cell voltage but caused carbon deposition at the cell inlet. The voltage increase seemed not to be affected by H_2S or HCl, and no acetic acid was measured at the cell outlet, indicating that these contaminants do not affect the primary tar conversion.

KEYWORDS

biomass gasifier, contaminants cross-influence, direct internal tar reforming, H_2S, HCl, SOFC

1 | INTRODUCTION

Electricity and heat production accounts for the 25% of global greenhouse gas emissions.[1] Integrated biomass gasifier solid oxide fuel cell systems might represent an alternative to fossil-fuel-based combined heat and power (CHP) generators, thus reducing carbon dioxide emissions in the atmosphere. The low energy density and scattered distribution of biomass make it is necessary to develop small-scale systems to exploit the biomass potential sustainably.

Among the various gasification technologies, updraft gasifiers are suitable for this application since they can handle different types of biomass in terms of moisture and size, emit low amounts of particulate matter, and have high cold gas efficiency.[2] Therefore, they can be fed with both energy crops, that is, plantations grown specifically for energy production, and residual waste streams, including by-products from agriculture, forestry, farm, and agro-industry. However, updraft gasifier biosyngas contains large amounts of light condensable compounds, volatile organic compounds, and tar (around 150 g/Nm^3 dry basis[2]). These compounds might create several issues as plugging filters pores, gas lines and heat exchangers, deactivation of catalysts, and condensation in cold spots and even at high temperature if polymerization occurs. However, these

compounds might act as fuel in the SOFC, and due to the endothermicity of reforming reactions, they could reduce the excess cathode air required to maintain constant the SOFC temperature, thus increasing the system efficiency. Moreover, avoiding or simplifying the tar cleaning step reduces system complexity and costs, thus facilitating the technology entry in the market.

The SOFC operating temperature, the presence of Ni catalyst, steam, and carbon dioxide in the inlet gas stream as well as generated at the triple phase boundary make direct internal reforming, that is, the reforming of tar and hydrocarbons directly in the anode chamber, theoretically possible. Various authors have investigated with experimental work the feasibility of direct internal reforming. Usually, model tar compounds are used in these studies. Toluene is probably the most used model tar compound.[3-9] However, also naphthalene[10-12] and benzene[13,14] are used. Only few works can be found with primary tar (eg, methanol, ethanol, acetic acid, and hydroxyacetone), and they are mostly focused on direct utilization and not on primary tar as biosyngas contaminants.[15-17] These compounds are called tar despite they generally have a molecular weight lower than that of benzene. They are the first compounds released during biomass pyrolysis and gasification, and they further evolve to form secondary and tertiary tar, such as toluene, naphthalene, and coronene.[18]

At present, there is not yet general agreement on the fate of tar in SOFC. Papurello et al reported an irreversible increase in the low frequency range impedance spectra of a Ni-YSZ cell fed with simulated biosyngas and an amount of toluene as low as 0.1 g/Nm^3.[19] Pieratti et al coupled a cocurrent fixed bed biomass steam gasifier with two SOFC stack. A filter with calcined dolomite and manganese oxide supported on zirconium silicate was used for tar and H_2S removal. After a short period of time, the stack performances decreased, may be due to the insufficient dimension of the filter.[20] On the other hand, Baldinelli et al indicated that 10 g/Nm^3 toluene in a simulated biosyngas mixture on Ni-YSZ did not harm the cell and no carbon was observed in postmortem analysis.[21] Some groups have carried out short-term tests with biosyngas from an autothermal downdraft gasifier and from an allothermal bubbling fluidized bed gasifier with real tar up to 3 g/Nm^3. Despite the presence of tar, a Ni-GDC anode cell fed with the gas showed continuous stable performance. However, in a test where biosyngas particulate reached the cell, postmortem SEM analysis identified carbon-based tubular structures in the anode functional layer.[22] Hofmann et al integrated a circulating fluidized bed biomass gasifier with a single cell test station. They measured a stable performance when feeding a Ni-GDC cell with biosyngas containing 10 g/Nm^3 tar.[23] Long-term tests with single cells and stack tests using real tar are however still required.

Biosyngas contains other minor species, among which H_2S and HCl, that can harm the SOFC and negatively affect the catalytic reactions occurring in the anode chamber. The effects of H_2S have been widely studied with different fuels, anode materials, and operating conditions. With Ni-YSZ anode cells, when H_2 is the fuel, H_2S is adsorbed on Ni active sites partially inhibiting electrochemical reactions.[24] Ni coverage causes a sudden drop in the cell operating voltage.[25] This is followed by a quasi-steady state voltage,[26] or by a slow degradation.[27] The higher the H_2S concentration, the more severe the drop. Rasmussen and Hagen indicated that for an anode-supported Ni-YSZ cell under load at 850°C, saturation coverage is reached around 40 ppm(v) H_2S.[28] Norheim et al indicated 80 ppm(v) H_2S at 800°C.[29] The effect was reversible and decreased with increasing operating temperature.[30] The presence of steam seems to help the desorption of adsorbed sulfur.[31] Different authors reported contradicting results on the effects of current density, with some suggesting a beneficial effect[32] and some a worsening impact.[33] Analysis of Ni-YSZ anode cell impedance indicated that H_2S causes an increase in the cell polarization at high frequency, which was ascribed to charge transfer process. However, at low hydrogen partial pressure, also the low frequency part of the cell polarization resistance was affected.[34] Ni-GDC anodes seem more tolerant to sulfur poisoning, due to the large surface area of ceria remaining active for electrochemical reactions.[12] For H_2S concentrations higher than 0.1% in volume, sulfur can react with the anode material.[35] However, Dong et al detected Ni_3S_2 using Raman Spectroscopy for the analysis of a cell contaminated with only 100 ppm(v) H_2S.[36] The formation of sulfur compounds is considered responsible for irreversible cell performance degradation.[37]

When carbon-containing fuels are used, H_2S might affect also the catalysis of reforming and water-gas shift reactions.[38] Rasmussen indicated that in a Ni-YSZ anode-supported cell fed with a mixture of $CH_4/H_2/H_2O$ and operated at 850°C, 4 ppm(v) H_2S has a larger effect on reforming than on electrochemical activity, with more than 60% of the reforming activity suppressed.[39] In fact, as reported by Rostrup-Nielsen, the sites for reforming and electrochemical reactions are different.[40] Similarly, Hagen observed an increase in both the high and low frequency range of a Ni-YSZ impedance spectra fed with $H_2/H_2O/CO$ and 2-9 ppm(v) H_2S. The increased H_2 diffusion resistance was ascribed to poisoning of the water-gas shift reaction.[41] Cells with Ni-ScSZ anodes are reported to have better sulfur tolerability,[42] that is, outrun by Ni-GDC anodes, which remain active for H_2 and CO electrochemical oxidation[43] and are reported to be active toward catalytic CH_4 reforming.[44] In addition to methane reforming, Sasaki et al studied the effect of H_2S on ethane, propane, butane, and iso-octane with Ni-ScSZ cells. They found that 3 ppm(v) H_2S accelerates carbon deposition due to the suppression of reforming.[24] Seemingly contradictory results were obtained by Boldrin et al when investigating toluene reforming on Ni-GDC composites. The presence of H_2S above 11 ppm(v) resulted in a decrease in the carbon formation.[45]

Also, the effect of HCl contamination on SOFC anodes has been investigated in the past years.[12,46-50] According to equilibrium calculations, HCl reacts with Ni forming $NiCl_x$. These compounds are gaseous at SOFC operating conditions, and their concentration increases fast with low HCl amount and is almost stable at high HCl amount.[51] The poisoning effect is believed to be due to the formation and subsequent sublimation of $NiCl_2$, as observed by Sasaki et al using Cl_2 as chlorine precursor.[24] Experimental results showed that poisoning by low HCl concentration is reversible.[52] At low concentrations in hydrogen feed, Aravind et al found that 9 ppm of HCl does not affect the performance of cells with Ni-GDC anodes. Similarly, Li et al and Błesznowski et al reported that a Ni-YSZ anode-supported cell can tolerate up to 10 ppm of chlorine on short-term operation at 750°C.[12,53] At concentrations higher than 100 ppm, Haga et al observed an only partially recoverable degradation that was ascribed to adsorption on active sites and sublimation of $NiCl_2$.[49] Kuramoto et al found that Ni-YSZ cells operated at 900°C with a current density of 150 or 200 mA/cm^2 were not affected by the presence of 10 ppm(v) HCl when fed with simulated post-CCS syngas ($H_2/N_2/H_2O$ = 70.9/23.6/5.5 vol%).[26]

A different and faster degradation mechanism takes place when a carbon-containing fuel is used compared to hydrogen. Marina et al reported that the presence of 50-800 ppm HCl in coal syngas causes immediate and reversible minor power losses in SOFC. The authors attributed the losses to the contaminant adsorption on Ni, thus blocking its electrocatalytic activity.[46] Trembly et al tested Ni-YSZ button cells at 800°C with simulated coal syngas and observed performance losses right after the injection of the contaminant even at concentrations as low as 20 ppm; they explained the poisoning effect of HCl with adsorption and blocking of the active sites.[50] Conversely, Bao et al observed no significant degradation when feeding an electrolyte-supported Ni-YSZ cell with 40 ppm HCl.[54] Xu et al observed with SEM a morphological change in the surface of Ni particles that were more scabrous after exposing the cell to syngas with 100 ppm HCl. Despite no significant performance loss, the presence of HCl might cause long-term degradation and also cause wear and corrosion of other parts made of stainless steel.[47] Recent studies carried out by Reeping et al with Ni-YSZ cells operated at 700°C with methane as fuel and 100-300 ppm HCl resulted in rapid cell performance degradation. Adsorbed HCl blocked at least part of the nickel active sites for CH_4 adsorption while hydrogen continued to dissociate and diffuse to the TPB. At higher temperatures, the cell degraded less but the degradation was irreversible due to the sublimation of $NiCl_x$.[55] Conversely, Madi et al reported more sever degradation when the cell was fed with H_2 rather than with syngas. They explained the observation by the decrease in HCl adsorption as due to competitive CO adsorption and oxidation.[56] Papurello et al showed that below 20 ppm(v) a cell fed with biogas reformate does not suffer degradation, and below 40 ppm(v) there is only a slight influence on the electrochemical processes occurring at the anode. Above this concentration, the loss in performance was considered to be probably caused by HCl adsorption on Ni.[19] Despite the presence of publications on the topic, there is no unanimity on the tolerance level indicates the necessity to carry out more studies.

Direct internal tar reforming might cause carbon deposition and failure due to thermal and mechanical stress.[57] Despite the presence of some literature on direct internal tar reforming, not sufficient research is available on the impact of biosyngas primary tar on SOFC. Moreover, excluding the studies of Sasaki et al on copoisoning of H_2S and hydrocarbons,[24] and Papurello et al[19] and Boldrin et al[45] on cross-influence of sulfur and toluene, the effect of H_2S on tar reforming and in particular on primary tar has not been investigated. The same holds for the cross-influence of HCl and tar, with exception for a previous work where toluene was used as tar.[58] Furthermore, there is no agreement on the effect of HCl on catalytic reactions involving methane and carbon monoxide. The aim of this study was therefore to investigate the cross-influence of acetic acid, H_2S, and HCl on the anode of solid oxide fuel cells. A commercial electrolyte-supported Ni-GDC SOFC was fed with simulated biosyngas and known concentrations of acetic acid, H_2S, and HCl separately. Successively, the cross-influence of the tar with one of the other two contaminants was studied. SOFC tolerance limits to tar, H_2S, and HCl are not yet well defined and are based on single contaminant effects. The results are expected to help the design of integrated biomass gasifier SOFC systems and therefore facilitate the development of this technology.

2 | METHODOLOGY

In the present study, we used simulated biosyngas to evaluate the effect of H_2S and HCl on primary tar reforming, as well as on CH_4 reforming and water-gas shift (WGS) reactions in an operating Ni-GDC SOFC. As reported in literature, tar and biosyngas components might compete for anode active sites, and therefore, the effect of tar is more thoroughly discerned under syngas.[45] A representative updraft biomass gasifier composition was taken from literature.[59] The H_2S concentrations tested were 0.8 and 1.3 ppm(v) dry basis, while for HCl 3.4, 20, and 50 ppm(v) dry basis were tested. The H_2S and HCl concentrations were selected based on SOFC tolerance limits found in literature.[60] Acetic acid was selected as primary tar, since it is one of the most abundant light condensable species generated from updraft gasifiers.[18] The concentration of acetic acid was varied from 17 to 128 g/Nm^3 dry basis, which is roughly the expected tar amount from updraft gasification.[2] The experimental campaign was conducted using three different cells: cell 1 to test the effect of tar alone

(test 1.1-1.4), cell 2 to test the effect of H_2S first (test 2.1 and 2.2) and then the cross-influence of H_2S and acetic acid (test 2.3 and 2.4), and cell 3 to test HCl first (test 3.1-3.3) and then HCl and acetic acid simultaneously (test 3.4-3.7). Thermodynamic equilibrium calculations were performed using the software FactSage version 5.4.1 (Thermfact/CRCT and GTT-Technologies) to calculate the required amount of water to avoid carbon deposition at 400°C, that is, the assumed operating temperature of a gas cleaning unit being developed by TU Delft and HyGear in FlexiFuel-SOFC project[61] for removing H_2S around the ppm(v) level. The software takes as inputs the mass of the reactants, process temperature, and pressure and gives as outputs the products and their amounts based on Gibbs free energy minimization.[62]

2.1 | Setup and equipment

A scheme of the test station used in this study is illustrated in Figure 1. A ceramic housing with platinum gauzes as current collectors on both anode and cathode sides was positioned in a temperature controlled furnace. A weight of 10 kg on top of the housing was used to assure contact between electrodes and current collector, and to improve the anode chamber sealing that was achieved using gaskets of Thermiculite™ 866. Electrolyte-supported cells (HC Starck) with 100 µm thick electrolyte, 40 µm anode, and 44 µm cathode were used. The anode was made of Ni-GDC and the cathode LSM mixed with 8YSZ; both electrodes had an area of 81 cm^2. The electrolyte was 8YSZ and had an area of 100 cm^2. The flow rates were regulated using Mass Flow Controllers (MFC) Bronkhorst EL-FLOW F201C (Bronkhorst). Steam was added to the fuel gas stream using a Controlled Evaporation Mixing (CEM) unit W202A (Bronkhorst). Acetic acid of 99.7% purity (Sigma Aldrich) was added using a peristaltic pump BT100-2J (Longer Precision Pump Co.). The liquid acetic acid was evaporated by trace heating the pipe where the contaminant was injected. The stainless steel pipes after the CEM and the acetic acid injection were trace heated to 150°C. Hydrogen sulfide was added using a gas bottle containing 500 ppm(v) of the contaminant in N_2 while for HCl a bottle containing 300 ppm(v) in N_2 (Linde). A polytetrafluoroethylene pipe was used for connecting the gas bottles with the MFC and this with the anode inlet as close as possible to the furnace to avoid any interaction with the stainless steel piping. The polarization (i-V) curves were recorded using an external load PLZ603W (Kikusui Electronics Corp.) and a DC power supply SM120–25D (Delta Elektronika BV). The open circuit voltage (OCV) measured was compared with the Nernst voltages calculated using Equation 1 below

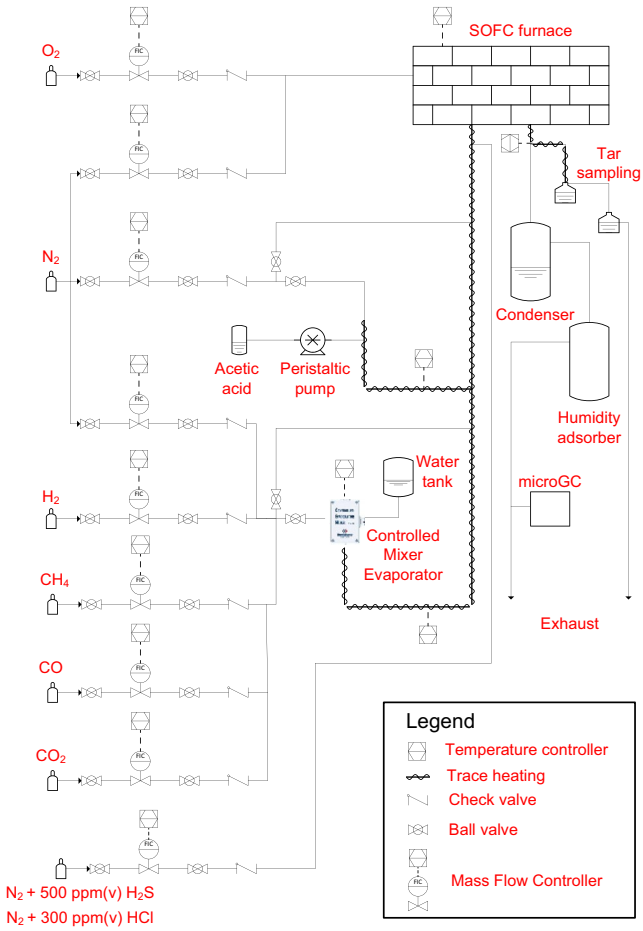

FIGURE 1 Scheme of the test station

$$V_{\text{Nernst}} = \frac{RT}{4F} \ln\left(\frac{P_{O_{2\text{cat}}}}{P_{O_{2\text{ano}}}}\right) \quad (1)$$

where R is the universal gas constant, T is the cell operating temperature, F is the Faraday constant, and P_{O_2} the equilibrium oxygen partial pressure at cathode and anode sides calculated using FactSage. A microGC Agilent 490 with a CP-Molsieve 5Å capillary for measuring CO, H_2, N_2, and CH_4 and a PoraPlot U capillary for measuring CO_2 (Agilent) was used to measure the outlet gas composition. Before reaching the microGC, the gas was passed through a condenser and a desiccator containing silica gel to remove the moisture contained in the gas. The anode outlet flow rate was back-calculated from the inlet N_2 flow rate and the N_2 outlet concentration measured with the microGC. This was then used to calculate the flow rates of H_2, CO, CO_2, and CH_4. The results are used for a qualitative analysis of the trends observed at different operating conditions. The isopropanol used for tar sampling was analyzed with a Varian 430 GC-FID (Agilent).

2.2 | Testing procedure

After having reduced the cell at 950°C by stepwise replacing with H_2 the total anode flow rate of 1500 NmL/min N_2 used during heating up, the furnace temperature was lowered to

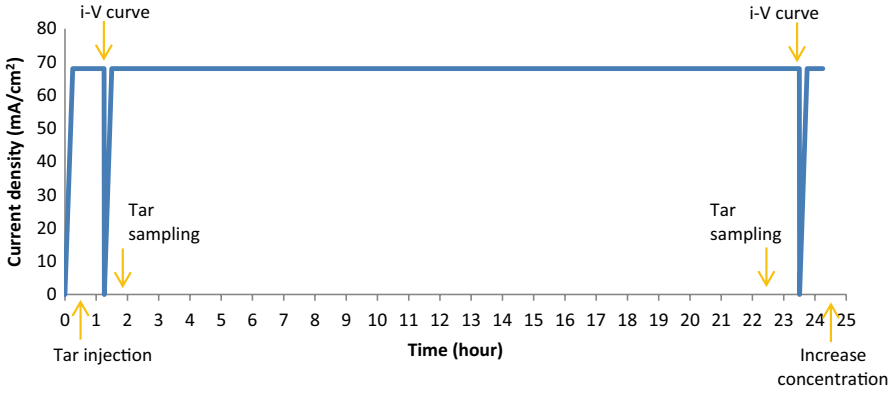

FIGURE 2 Example of the testing procedure followed for the first concentration of acetic acid tested

obtain a cell temperature of 800°C. An anode flow rate of 1000 NmL/min composed of 15% H_2, 20% CO, 15% CO_2, 2% CH_4, and 48% N_2 and a cathode flow rate of 3000 NmL/min simulated air were used. Each contaminant concentration was maintained for 24 hours. In the H_2S test, after the first 24 hours of exposure to the contaminant, the cell was operated for 24 hours under load with clean biosyngas to verify eventual recovery. In all the tests, the cells were operated at 800°C and nearly atmospheric pressure with a current of 68 mA/cm^2. The outlet gas composition was measured continuously during the tests; i-V curves were recorded with clean biosyngas, and at the beginning and at the end of the exposure to each contaminant concentration. When measuring i-V curves, the current was varied only between 0 A (Open Circuit) and the operating current kept during the contaminant exposure. The amount of acetic acid at the cell outlet was measured by bubbling the gas in two impinger bottles in series containing isopropanol at room temperature and at 0°C, respectively. The sampling was carried out at the beginning and at the end of the injection of acetic acid, as illustrated in Figure 2.

After having performed the test with H_2S, the cell temperature was increased to 950°C and the anode gas composition was changed to pure H_2. The cell was kept at open circuit for 12 hours before decreasing the temperature to 800°C and changing the anode gas to biosyngas. The same cell was used to test the cross-influence of acetic acid and H_2S. The cell was first exposed to 42 g/Nm^3 acetic acid; then also, 0.8 ppm(v) H_2S was added. Acetic acid was then removed, and the cell was kept with H_2S only for five hours. Also after testing HCl alone, the cell was kept at OCV at 950°C with pure H_2 for 12 hours. The temperature was then decreased to 800°C and the anode flow changed to simulated biosyngas. Successively, 42 g/Nm^3 acetic acid was added for 24 hours before adding an increasing amount of HCl, with each concentration kept for 24 hours. The flow of acetic acid was stopped 90 minutes

TABLE 1 Synoptic table summarizing the tests performed and the relevant parameters

Cell #	Test #	H_2S concentration (ppm(v) d.b.)	HCl concentration (ppm(v) d.b.)	Tar concentration (g/Nm^3)/(ppm(v))	Operating conditions (mA/cm^2)	Duration (h)
1	1.1	/	/	17/6526	68	24
	1.2	/	/	41/15 743	68	24
	1.3	/	/	83/31 534	68	24
	1.4	/	/	128/47 863	68	24
2	2.1	0.8	/	0	68	24
	2.2	1.3	/	0	68	24
	2.3	0	/	42/16 789	68	24
	2.4	0.8	/	42/16 789	68	24
3	3.1	/	3.4	0	68	24
	3.2	/	20	0	68	24
	3.3	/	50	0	68	24
	3.4	/	0	42/16 789	68	24
	3.5	/	3.4	42/16 789	68	24
	3.6	/	20	42/16 789	68	24
	3.7	/	50	42/16 789	68	24

after having removed the last concentration of HCl tested. Table 1 summarizes the tests performed and the relevant operating conditions.

3 | RESULTS AND DISCUSSION

Equilibrium calculations indicated that to avoid carbon deposition at 400°C, taking as input the selected gas composition and 150 g/Nm^3 of acetic acid, it is necessary to add 0.47 g of water per normal liter of dry gas, corresponding to a volume flow rate of 584 NmL/min. Figure 3 shows the cells performances at 950°C with dry H_2, and at 800°C with dry and wet H_2 as well as with biosyngas.

Table 2 shows the cell anode flow rates set at the cell inlet, measured at the cell outlet, and the equilibrium composition calculated using FactSage. The gas composition was measured during the operation of the cell with 68 mA/cm^2; therefore, the additional oxygen flow reaching the anode was considered for calculating the equilibrium composition. Methane was not completely reformed in the cell anode. Therefore, also H_2 and CO flow rates were lower than the expected equilibrium values. The incomplete reforming might explain the difference between OCV measured and calculated using Nernst equation. As shown in Table 3, the OCV calculated replacing 8 NmL/min of methane with an inert gas (ie, considering that 8 NmL/min of methane do not react in the anode chamber) is very close to the measured value. A lower OCV could be due also to gas leakages. However, comparing the calculated and measured OCV with humidified hydrogen, the sealing of the cell appeared as decent.

3.1 | Test with acetic acid: cell 1 test 1.1-1.4

Figure 4 shows the OCV measured and calculated with the different concentrations of acetic acid tested. The presence of acetic acid resulted in an increase in the cell OCV, thus indicating that the primary tar was converted into fuel. However, the measured OCV was lower than the calculated values. Therefore, not all the acetic acid injected was converted into usable fuel.

The presence of acetic acid resulted in an increase in H_2, CO, CO_2, and also CH_4 outlet flow rates. An increase in methane might indicate that acetic acid somewhat hinders methane reforming, or that it is converted at least partly via thermal decomposition rather than catalytic reforming. Interestingly, the cell temperature decreased from 793°C to 790°C when 128 g/Nm^3 acetic acid was present. The endothermic reforming of acetic acid might be responsible for the temperature decrease, but also the increased anode flow rate might have caused this effect. While the amount of CO_2 measured was equal to the expected equilibrium amount, the measured flow rates of CO and H_2 were lower than the equilibrium ones. This is in agreement with the lower OCV measured as compared to the calculated one. No acetic acid was measured at the cell outlet by tar sampling. Only with the highest concentration of acetic acid tested, that is, 128 g/Nm^3, traces (below 1 g/Nm^3 dry basis) of hydroxyacetone were measured. Therefore, acetic acid was completely converted. At the end of the test, a significant amount of carbon was present in the cell inlet ceramic pipe, at the inlet of the ceramic housing, and in a minor amount on the anode surface close to the inlet. The carbon deposited on the cell might have been formed in the inlet pipes and entrained by the gas or might be the result of incomplete catalytic reforming.

Even the highest concentration of acetic acid seemed to be completely converted. However, this compound caused severe carbon deposition. The formation mechanism is not completely clear. In a biomass gasifier SOFC system, severe carbon deposits could cause plugging of pipes and reactors. Large amount of acetic acid should therefore be considered as a contaminant in systems operating at these conditions, unless appropriate conditions for preventing the cracking of this hydrocarbon before it reaches the anode are adopted. Nonetheless, this compound is a valuable fuel and it would be

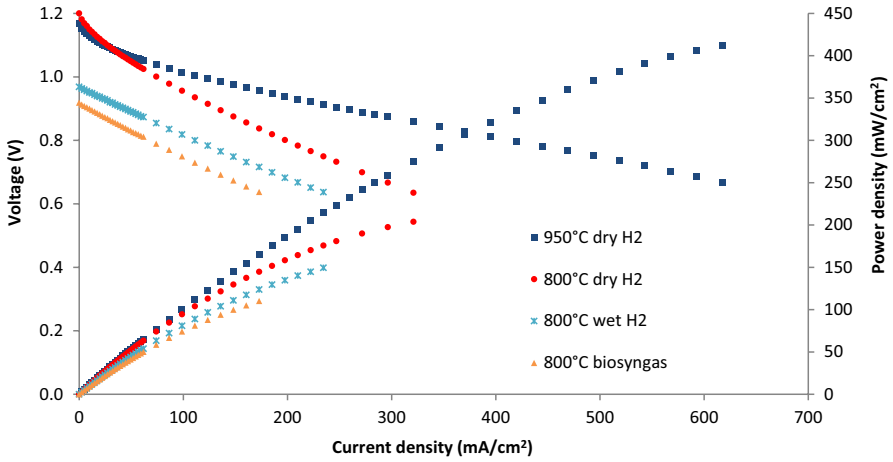

FIGURE 3 Cell polarization and power density curves after cell reduction with dry and wet H_2, and with biosyngas

TABLE 2 Inlet, outlet, and equilibrium anode flow rates

Flow rate [NmL/min]	H_2	N_2	CH_4	CO	CO_2
Inlet	150	433	20	200	150
Equilibrium	272	433	0	120	250
Outlet measured	242	433	8	114	247

TABLE 3 Comparison between calculated and measured OCV with biosyngas and with humidified hydrogen

OCV calculated	OCV measured	Deviation [%]	Gas composition
0.922	0.919	−0.41	Biosyngas equilibrium composition
0.919	0.919	−0.03	Biosyngas lack of complete reforming
0.967	0.967	−0.02	Humidified H_2

preferable to convert it into H_2 and CO rather than removing it from the gas stream.

3.2 | Tests with H_2S: cell 2 test 2.1-2.4

In the test with hydrogen sulfide, the presence of the contaminant caused an immediate and significant voltage drop, as visible from the open circuit voltage values presented in Table 4, in agreement with literature.[28] The 24-hour recovery between the tests with 1.3 ppm(v) and 0.8 ppm(v) H_2S allowed an almost complete recovery of the cell OCV. Sulfur poisoning is considered reversible for concentrations lower than 100 ppm(v) and temperature above 600°C.[63] However, the 7-hour period after the addition of 0.8 ppm(v) H_2S resulted in an incomplete recovery. This might have been due to an insufficient recovery time rather than an irreversible poisoning, since the concentration tested was even lower than the previous one.

TABLE 4 OCV measured with different H_2S concentrations and after recovery

	OCV measured (V)	OCV drop/increase (%)
Biosyngas	0.908	
1.3 ppm(v) H_2S	0.883	−2.8
Biosyngas	0.907	2.8
0.8 ppm(v) H_2S	0.884	−2.6
Biosyngas	0.902	2.1

The analysis of the gas composition at the outlet helps understanding the causes of the decreasing OCV. The flow rates of CH_4 and CO increased while those of H_2 and CO_2 decreased, as visible from the values presented in Table 5. In fact, the presence of H_2S prevented methane steam reforming, as reported in,[42] and partially hindered WGS reaction, as suggested in Refs.[41,64,65]

After the 12-hour recovery period at 950°C with pure H_2, the cell was again fed with biosyngas, and after 24 hours of operation, the test on the cross-influence of acetic acid and H_2S started. The anode outlet flow rates are presented in Figure 5. As noticed during the previous test, adding acetic acid resulted in an increase in H_2, CO, CO_2, and CH_4 outlet flow rates, in addition to the OCV increase. Moreover, when also 0.8 ppm(v) H_2S was added at the inlet flow, methane reforming was completely prevented and WGS partially hindered. Interestingly, when both contaminants were present, the amount of methane at the cell outlet was higher than the inlet set value. Moreover, when the flow of acetic acid was stopped, there was a clear decrease in the outlet flow rates of H_2, CO, and CO_2. This shows that part of the acetic acid undergoes thermal decomposition

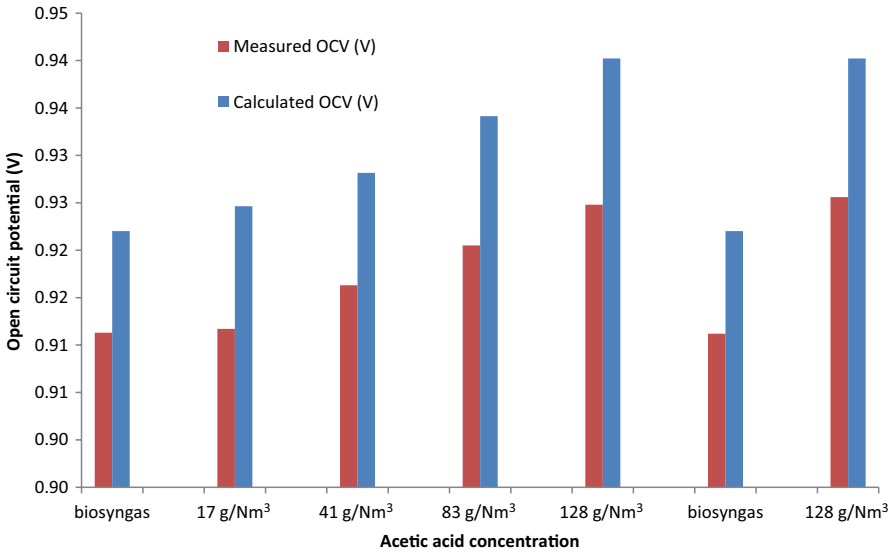

FIGURE 4 Comparison between calculated and measured OCV with different acetic acid concentrations (cell 1, Test 1.1-1.4)

TABLE 5 Inlet, equilibrium, and measured outlet anode flow rates with clean biosyngas and with 0.8 ppm(v) H_2S

Flow rate [NmL/min]	H_2	N_2	CH_4	CO	CO_2
Inlet	150	433	20	200	150
Equilibrium	272	433	0	120	250
Outlet measured biosyngas	226	433	9	115	244
Outlet measured 0.8 ppm(v) H_2S	129	433	21	180	172

rather than being fully catalytically reformed, according to the reactions presented in Ref.[66]:

$$CH_3COOH \rightarrow 2CO + 2H_2 \quad (2)$$

$$CH_3COOH \rightarrow CH_4 + CO_2 \quad (3)$$

$$CH_3COOH \rightarrow C_2H_4, C_2H_6, C_3H_4, \text{coke}, \ldots \quad (4)$$

The OCV values presented in Table 6 also show that H_2S does not significantly affect acetic acid conversion. The removal of acetic acid caused a voltage drop close to the voltage gain measured when acetic acid was initially added. Tar sampling at the cell outlet did not show the presence of acetic acid or other compounds, thus confirming that the primary tar was fully converted.

In summary, the presence of around 1 ppm(v) H_2S caused a voltage drop due to the inhibition of methane and water-gas shift reaction. However, the effect was reversible. H_2S does not significantly affect acetic acid conversion. In a biomass gasifier SOFC system, hindering WGS is not necessarily a drawback. Before reaching the SOFC, the biosyngas passes through a gas cleaning unit. If ZnO-CuO are used for sulfur removal at 400°C, the WGS reaction is catalyzed by the sorbents and its equilibrium is highly shifted toward the product. Since SOFC operates at temperatures higher than 400°C and the WGS is an exothermic reaction, inside the SOFC reverse WGS would happen, thus decreasing the availability of fuel. Differently, the negative effect H_2S has on methane reforming might result in fuel starvation in systems operating without an external reformer. Therefore, despite literature indicates that oxidation reactions are less affected than WGS and CH_4 reforming,[67] the effect H_2S has on these two reactions should be taken into account when considering a SOFC heat and fuel management.

3.3 | Tests with HCl: cell 3 test 3.1-3.7

The presence of hydrogen chloride did not appear to cause a significant effect on the anode catalytic reactions, as visible from the open circuit voltage values presented in Table 7, which decrease by only 4 mV when HCl was present.

After the 12-hour recovery period at 950°C with pure H_2, the anode gas feed was again changed to biosyngas to test cross-influence of acetic acid and HCl. Table 8 shows the average outlet flow rates measured during the test.

As noticed during the test with cells 1 and 2, acetic acid caused an increase in H_2, CO, and CO_2 outlet flow rates. Also CH_4 outlet flow rate increased, despite only marginally.

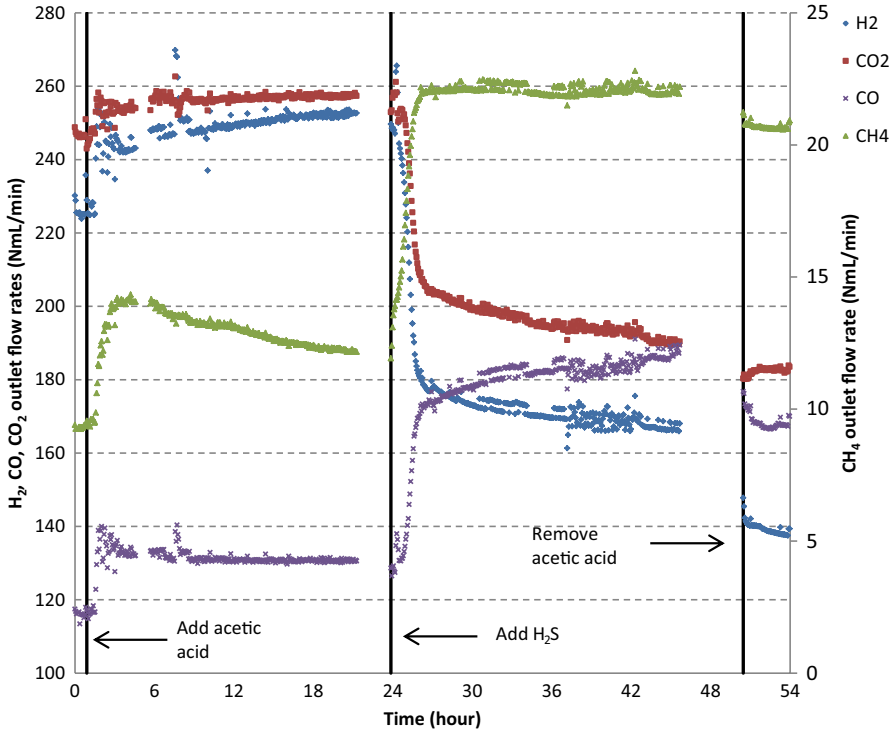

FIGURE 5 Outlet flow rates measured when studying the cross-influence of acetic acid and H_2S (cell 2, Test 2.3-2.4)

TABLE 6 Measured OCV and percentage drop or increase due to the presence of acetic acid and H_2S

	OCV measured (V)	OCV drop/ increase (%)
Biosyngas	0.904	
Tar	0.911	0.8
Tar + H_2S	0.890	−2.3
H_2S	0.884	−0.6
Biosyngas	0.906	2.5

When HCl was added, the outlet flow rates did not change substantially, thus indicating that HCl seems not to affect acetic acid conversion significantly. Tar sampling at the cell outlet did not show the presence of acetic acid or other compounds. Moreover, as noticed in the tests with HCl alone, WGS and methane steam reforming reactions seem not to be heavily affected by the presence of chlorine as observed in the case of H_2S.

This result is different from some conclusions reported in literature. Marina et al and Trembly et al observed an immediate performance drop of a Ni-YSZ cell operating at 800°C with syngas when 50 and 20 ppm HCl were added to the anode feed. The performance drop was attributed to the contaminant affecting the cell electrocatalytic activity, in accordance with studies on methane reforming and water-gas shift reaction with nickel catalysts by Richardson et al.[46,50,68] Nonetheless, the authors did not measure the outlet gas composition and there is therefore no direct observation of the phenomenon. Upon checking the gas composition with thermodynamic equilibrium calculations, it can be noticed that in both cases, the anode inlet composition was not at equilibrium at the cell operating temperature and HCl might have hindered WGS reaction. Since the syngas composition used did not contain any CH_4, no information on the effect of HCl on direct methane reforming can be obtained. Reeping et al indicated that in a cell operating at 700°C with CH_4, HCl inhibits CH_4 reforming on the Ni catalyst.[55] Also in this case, the gas outlet composition was not measured but the observation was derived from operando in situ and ex situ optical methods. The lower operating temperature and the higher chlorine concentration in Reeping et al experiments might explain the difference with the present study.

TABLE 7 OCV measured with different HCl concentrations and after recovery

	OCV measured (V)	OCV drop/ increase (%)
Biosyngas	0.911	
3.4 ppm(v) HCl	0.907	−0.4
20 ppm(v) HCl	0.907	0.0
50 ppm(v) HCl	0.906	−0.1
Biosyngas	0.907	0.1

The results presented in this manuscript are however in agreement with other studies available in literature. In a study by Madi et al, anode-supported Ni-YSZ cells operating at 750°C with simulated syngas (CH_4 0.3%, CO_2 10%, CO 19.3%, H_2 50.6% and H_2O 19.9%) showed no voltage drop when 10 to 90 ppm(v) HCl were added. However, when calculating the expected thermodynamic equilibrium gas composition, it is noticed that the inlet gas composition used was equal to the equilibrium composition at cell operating temperature, and HCl hindering CH_4 reforming would have caused a decrease in voltage of only 1 mV. By comparing the degradation of cells fed with HCl in H_2 or syngas, and observing no degradation in a stack fed with syngas and up to 500 ppm(v), the authors of the study suggested that CO might compete with HCl for Ni active sites thus acting as a protection for chlorine poisoning.[56] With a gas composition of 50.8% H_2, 19.5% CO, 9.1% CO_2, 0.7% CH_4, and 19.9% H_2O, Papurello et al measured the cell impedance spectra and observed no change in the charge transfer resistance of an anode-supported cell with up to 20 ppm(v) HCl. At higher contaminant concentrations, the effect of the contaminant was mostly visible on the high frequency resistance associated with charge transfer process. However, also in this study, the inlet gas composition used was already at equilibrium at the cell operating temperature of 750°C.[19] Also, Xu et al observed no voltage drop when 100 ppm HCl was added to simulated syngas with 30% H_2, 26% H_2O, 23% CO, and 21% CO_2. Similar to the previous studies, the gas inlet composition was very close to the equilibrium composition expected at the cell operating temperature. Therefore, no information on the contaminant effect on Ni catalytic activity can be obtained. Nonetheless, there was no significant performance loss visible from the impedance spectra analysis.[47] Also, Bao et al observed no voltage drop and no degradation of a Ni-YSZ cell during a 100-hour test at 750°C and 800°C with 40 ppm HCl in a gas mix of 30.6% H_2, 30.0% CO, 27.6% H_2O, and 11.8% CO_2.[54] In this case, the gas inlet composition was not at equilibrium at the cell operating temperature. Therefore, it appears that water-gas shift reaction was not hindered by the presence of chlorine.

In our previous tests reported in,[58] we studied the cross-influence of toluene and HCl on a Ni-GDC SOFC fed with hydrogen, and HCl appeared to affect the reforming of toluene. The different behavior observed with toluene and acetic acid can be due to the higher reactivity of acetic acid. This compound in fact might undergo at least partially thermal decomposition rather than catalytic reforming; thus, HCl does not necessarily affect its conversion. In the same study, we observed the formation of methane when toluene was present in the gas feed, and an increase in the outlet CH_4 flow rate when

TABLE 8 Measured outlet anode composition with clean biosyngas, acetic acid, and acetic acid plus hydrogen chloride

Flow rate [NmL/min]	H_2	N_2	CH_4	CO	CO_2
42 g/Nm^3 acetic acid + 3.4 ppm(v) HCl	264	431	9	134	259
42 g/Nm^3 acetic acid + 20 ppm(v) HCl	258	417	9	137	252
42 g/Nm^3 acetic acid + 50 ppm(v) HCl	255	395	9	136	250
42 g/Nm^3 acetic acid	260	433	9	138	256
Biosyngas	234	433	8	117	249

HCl concentration was raised from 8 to 42 ppm(v) HCl. The behavior was explained in light of Reeping et al findings, that is, HCl preventing methane reforming. The lower operating temperature (ie, 750°C in the experiments with toluene) and other factors associated with methane formation from toluene might have played a role in the process.[55,58]

In summary, a concentration of HCl up to 50 ppm(v) seems not to largely affect the catalytic reactions occurring in the anode of a Ni-GDC SOFC operating at 800°C. The contaminant does not affect the conversion of acetic acid. Based on these results, it might appear that HCl does not always require a significant cleaning effort and it is therefore possible to simplify the gas cleaning section of a biomass gasifier SOFC system. However, cross-influence studies of HCl and other tar species are required to determine HCl tolerance limits in systems with direct internal tar reforming. Furthermore, the long-term effect of the contaminant on the anode catalytic and electrochemical reactions should be further investigated. Large quantities of HCl might however cause corrosion in other downstream equipment, especially in the heat recovery section of a micro-CHP system. Therefore, the implications of having a simplified gas cleaning unit should be analyzed not only at cell but also at system level.

4 | CONCLUSIONS

Biosyngas contaminants can be a techno-economic bottleneck for the development of small-scale integrated biomass gasifier solid oxide fuel cell systems. Tar compounds are usually removed or reformed externally since there is not yet complete understanding of their fate in solid oxide fuel cell anode. The concentration of other biosyngas contaminants, such as H_2S and HCl, is decreased in the ppm(v) range. However, this range is based on single contaminant effects. This might result in incorrect understanding of solid oxide fuel cell tolerance limits and improper design of the system gas cleaning unit. Therefore, the aim of this study was to investigate the influence of acetic acid, H_2S, and HCl on the catalytic reactions occurring in the anode of Ni-GDC SOFCs.

The results presented clearly show that acetic acid is at least partially converted into useful fuel at SOFC operating conditions. Both thermal decomposition and catalytic reforming seem possible conversion mechanism. Severe deposition of carbon was observed at the inlet of the ceramic housing. The presence of H_2S in biosyngas appears to completely stop direct CH_4 internal reforming, even at concentrations as low as 0.8 ppm(v). This results in lower amount of fuel available for the cell electrochemical reactions. Moreover, H_2S partially hinders WGS reaction. Interestingly, the presence of H_2S seems not to affect the conversion of acetic acid. This, together with the carbon deposited before the anode chamber, indicates that at least part of acetic acid might be thermally decomposed even before reaching the SOFC anode. The presence of HCl in concentrations up to 50 ppm(v) seems not to heavily affect the anode catalytic reactions. This manuscript provides additional insights on the fate of acetic acid in SOFC anode and on the cross-influence of H_2S, HCl, and acetic acid. The results are expected to help the integration of biomass gasifiers and SOFC systems.

ACKNOWLEDGMENTS

This research was partially supported by the project "FlexiFuel-SOFC." The project has received funding from the European Union's Horizon 2020 Research and Innovation Program under grant agreement No. 641229. The authors acknowledge Marco Graziadio for the help given in carrying out this work.

CONFLICT OF INTEREST

None declared.

NOMENCLATURE

ACRONYMS

CEM	Controlled evaporation mixing
CHP	Combined heat and power
DC	Direct current
EIS	Electrochemical impedance spectroscopy
GC	Gas chromatograph
GDC	Gadolinium-doped ceria
FID	Flame ionization detector
LSM	Lanthanum strontium manganite
MFC	Mass flow controller
OCV	Open circuit voltage
PTFE	Polytetrafluoroethylene

ScSZ	Scandia-stabilized zirconia
SEM	Scanning electron microscope
SOFC	Solid oxide fuel cell
TPB	Triple phase boundary
WGS	Water-gas shift
YSZ	Yttria-stabilized zirconia

SYMBOLS

F	Faraday constant (C/mol)
i	Current density (mA/cm^2)
$P_{O_{2cat}}$	Equilibrium oxygen partial pressure at cathode
$P_{O_{2ano}}$	Equilibrium oxygen partial pressure at cathode
R	Universal gas constant (J/mol*K)
T	Temperature (K)
V	Voltage (V)
V_{Nernst}	Nernst voltage (V)

ORCID

Alessandro Cavalli https://orcid.org/0000-0002-7548-0227

REFERENCES

1. IPCC. *Climate Change 2014: Mitigation of Climate Change. Contribution of Working Group III to the Fifth Assessment Report of the Intergovernmental Panel on Climate Change*. Cambridge, UK and New York, NY: IPCC; 2014.
2. Ud Din Z, Zainal ZA. Biomass integrated gasification-SOFC systems: technology overview. *Renew Sustain Energy Rev*. 2016;53:1356-1376.
3. Papurello D, Chiodo V, Maisano S, Lanzini A, Santarelli M. Catalytic stability of a Ni-Catalyst towards biogas reforming in the presence of deactivating trace compounds. *Renew Energy*. 2018;127:481-494.
4. Madi H, Diethelm S, Ludwig C, Van herle J. The impact of toluene on the performance of anode-supported Ni-YSZ SOFC operated on hydrogen and biosyngas. *ECS Trans*. 2015;68:2811-2818.
5. Liu M, Millan-Agorio MG, Aravind PV, Brandon NP. Influence of operation conditions on carbon deposition in SOFCs fuelled by tar-containing biosyngas. *J Electrochem Soc*. 2011;158:B1310-B1318.
6. Papurello D, Iafrate C, Lanzini A, Santarelli M. Trace compounds impact on SOFC performance: experimental and modelling approach. *Appl Energy*. 2017;208:637-654.
7. Liu M, van der Kleij A, Verkooijen A, Aravind PV. An experimental study of the interaction between tar and SOFCs with Ni/GDC anodes. *Appl Energy*. 2013;108:149-157.
8. Doyle TS, Dehouche Z, Aravind PV, Liu M, Stankovic S. Investigating the impact and reaction pathway of toluene on a SOFC running on syngas. *Int J Hydrogen Energy*. 2014;39:12083-12091.
9. Namioka T, Naruse T, Yamane R. Behavior and mechanisms of Ni/ScSZ cermet anode deterioration by trace tar in wood gas in a solid oxide fuel cell. *Int J Hydrogen Energy*. 2011;36:5581-5588.
10. Papurello D, Lanzini A, Leone P, Santarelli M. The effect of heavy tars (toluene and naphthalene) on the electrochemical performance of an anode-supported SOFC running on bio-syngas. *Renew Energy*. 2016;99:747-753.
11. Hauth M, Lerch W, König K, Karl J. Impact of naphthalene on the performance of SOFCs during operation with synthetic wood gas. *J Power Sources*. 2011;196:7144-7151.
12. Aravind PV, Ouweltjes JP, Woudstra N, Rietveld G. Impact of biomass-derived contaminants on SOFCs with Ni/Gadolinia-Doped ceria anodes. *Electrochem Solid-State Lett*. 2008;11:B24.
13. Mermelstein J, Brandon N, Millan M. Impact of steam on the interaction between biomass gasification tars and nickel-based solid oxide fuel cell anode materials. *Energy Fuels*. 2009;23:5042-5048.
14. Mermelstein J, Millan M, Brandon NP. The impact of carbon formation on Ni-YSZ anodes from biomass gasification model tars operating in dry conditions. *Chem Eng Sci*. 2009;64:492-500.
15. Leone P, Lanzini A, Ortigoza-Villalba GA, Borchiellini R. Operation of a solid oxide fuel cell under direct internal reforming of liquid fuels. *Chem Eng J*. 2012;191:349-355.
16. Lo Faro M, Stassi A, Antonucci V, et al. Direct utilization of methanol in solid oxide fuel cells: an electrochemical and catalytic study. *Int J Hydrogen Energy*. 2011;36:9977-9986.
17. Kaklidis N, Pekridis G, Besikiotis V, Athanasiou C, Marnellos GE. Direct electro-oxidation of acetic acid in a solid oxide fuel cell. *Solid State Ionics*. 2012;225:398-407.
18. Milne T, Abatzoglou N, Evans R. *Biomass Gasifier "tars": Their Nature, Formation, and Conversion*. Golden, CO: National Renewable Energy Laboratory; 1997.
19. Papurello D, Lanzini A, Drago D, Leone P, Santarelli M. Limiting factors for planar solid oxide fuel cells under different trace compound concentrations. *Energy*. 2016;95:67-78.
20. Pieratti E, Baratieri M, Ceschini S, Tognana L, Baggio P. Syngas suitability for solid oxide fuel cells applications produced via biomass steam gasification process: experimental and modeling analysis. *J Power Sources*. 2011;196:10038-10049.
21. Baldinelli A, Cinti G, Desideri U, Fantozzi F. Biomass integrated gasifier-fuel cells: experimental investigation on wood syngas tars impact on NiYSZ-anode solid oxide fuel cells. *Energy Convers Manag*. 2016;128:361-370.
22. Hofmann P, Panopoulos KD, Fryda LE, Schweiger A, Ouweltjes JP, Karl J. Integrating biomass gasification with solid oxide fuel cells: effect of real product gas tars, fluctuations and particulates on Ni-GDC anode. *Int J Hydrogen Energy*. 2008;33:2834-2844.
23. Hofmann PH, Panopoulos KD, Aravind PV, et al. Operation of solid oxide fuel cell on biomass product gas with tar levels >10 g Nm^{-3}. *Int J Hydrogen Energy*. 2009;34:9203-9212.
24. Sasaki K, Haga K, Yoshizumi T, et al. Chemical durability of solid oxide fuel cells: influence of impurities on long-term performance. *J Power Sources*. 2011;196:9130-9140.
25. Kavurucu Schubert S, Kusnezoff M, Michaelis A, Bredikhin SI. Comparison of the performances of single cell solid oxide fuel cell stacks with Ni/8YSZ and Ni/10CGO anodes with H2S containing fuel. *J Power Sources*. 2012;217:364-372.
26. Kuramoto K, Hosokai S, Matsuoka K, Ishiyama T, Kishimoto H, Yamaji K. Degradation behaviors of SOFC due to chemical interaction between Ni-YSZ anode and trace gaseous impurities in coal syngas. *Fuel Process Technol*. 2017;160:8-18.
27. Zha S, Cheng Z, Liu M. Sulfur poisoning and regeneration of Ni-based anodes in solid oxide fuel cells. *J Electrochem Soc*. 2007;154:B201.

28. Rasmussen J, Hagen A. The effect of H2S on the performance of Ni-YSZ anodes in solid oxide fuel cells. *J Power Sources*. 2009;191:534-541.
29. Norheim A, Wærnhus I, Broström M, Hustad JE, Vik A. Experimental studies on the influence of H2S on solid oxide fuel cell performance at 800 °C. *Energy Fuels*. 2007;21:1098-1101.
30. Matsuzaki Y. The poisoning effect of sulfur-containing impurity gas on a SOFC anode: part I. Dependence on temperature, time, and impurity concentration. *Solid State Ionics*. 2000;132:261-269.
31. Li TS, Miao H, Chen T, Wang WG, Xu C. Effect of simulated coal-derived gas composition on H_2S poisoning behavior evaluated using a disaggregation scheme. *J Electrochem Soc*. 2009;156:B1383.
32. Cheng Z, Zha S, Liu M. Influence of cell voltage and current on sulfur poisoning behavior of solid oxide fuel cells. *J Power Sources*. 2007;172:688-693.
33. Yoshizumi T, Uryu C, Oshima T, Shiratori Y, Ito K, Sasaki K. Sulfur poisoning of SOFCs: dependence on operational parameters. *ECS Trans*. 2011;35:1717-1725.
34. Lohsoontorn P, Brett D, Brandon NP. The effect of fuel composition and temperature on the interaction of H2S with nickel-ceria anodes for solid oxide fuel cells. *J Power Sources*. 2008;183:232-239.
35. Khan MS, Lee SB, Song RH, Lee JW, Lim TH, Park SJ. Fundamental mechanisms involved in the degradation of nickel–yttria stabilized zirconia (Ni–YSZ) anode during solid oxide fuel cells operation: a review. *Ceram Int*. 2016;42:35-48.
36. Dong J, Cheng Z, Zha S, Liu M. Identification of nickel sulfides on Ni-YSZ cermet exposed to H2 fuel containing H2S using Raman spectroscopy. *J Power Sources*. 2006;156:461-465.
37. Li TS, Wang WG, Chen T, Miao H, Xu C. Hydrogen sulfide poisoning in solid oxide fuel cells under accelerated testing conditions. *J Power Sources*. 2010;195:7025-7032.
38. Niakolas DK. Sulfur poisoning of Ni-based anodes for solid oxide fuel cells in H/C-based fuels. *Appl Catal A Gen*. 2014;486:123-142.
39. Rasmussen J, Hagen A. The effect of H2S on the performance of SOFCs using methane containing fuel. *Fuel Cells*. 2010;10:1135-1142.
40. Rostrup-Nielsen JR, Hansen JB, Helveg S, Christiansen N, Jannasch AK. Sites for catalysis and electrochemistry in solid oxide fuel cell (SOFC) anode. *Appl Phys A Mater Sci Process*. 2006;85:427-430.
41. Hagen A. Sulfur poisoning of the water gas shift reaction on anode supported solid oxide fuel cells. *J Electrochem Soc*. 2012;160:F111-F118.
42. Hagen A, Rasmussen J, Thydén K. Durability of solid oxide fuel cells using sulfur containing fuels. *J Power Sources*. 2011;196:7271-7276.
43. Ouweltjes JP, Aravind PV, Woudstra N, Rietveld G. Biosyngas utilization in solid oxide fuel cells with Ni/GDC anodes. *J Fuel Cell Sci Technol*. 2006;3:495.
44. Xu C, Zondlo JW, Gong M, Elizalde-Blancas F, Liu X, Celik IB. Tolerance tests of H2S-laden biogas fuel on solid oxide fuel cells. *J Power Sources*. 2010;195:4583-4592.
45. Boldrin P, Millan-Agorio M, Brandon NP. Effect of sulfur- and tar-contaminated syngas on solid oxide fuel cell anode materials. *Energy Fuels*. 2015;29:442-446.
46. Marina OA, Pederson LR, Thomsen EC, Coyle CA, Yoon KJ. Reversible poisoning of nickel/zirconia solid oxide fuel cell anodes by hydrogen chloride in coal gas. *J Power Sources*. 2010;195:7033-7037.
47. Xu C, Gong M, Zondlo JW, Liu X, Finklea HO. The effect of HCl in syngas on Ni-YSZ anode-supported solid oxide fuel cells. *J Power Sources*. 2010;195:2149-2158.
48. Bao J, Krishnan GN, Jayaweera P, Sanjurjo A. Effect of various coal gas contaminants on the performance of solid oxide fuel cells: part III. Synergistic effects. *J Power Sources*. 2010;195:1316-1324.
49. Haga K, Shiratori Y, Ito K, Sasaki K. Chlorine poisoning of SOFC Ni-Cermet anodes. *J Electrochem Soc*. 2008;155:B1233.
50. Trembly JP, Gemmen RS, Bayless DJ. The effect of coal syngas containing HCl on the performance of solid oxide fuel cells: investigations into the effect of operational temperature and HCl concentration. *J Power Sources*. 2007;169:347-354.
51. Aravind PV. Studies on high efficiency energy systems based on biomass gasifiers and solid oxide fuel cells with Ni/GDC anodes 2007.
52. EG&G Technical Service. *Fuel Cell Handbook*, 7th edn. Morgantown, WV: EG&G Technical Service; 2004.
53. Błesznowski M, Jewulski J, Zieleniak A. Determination of H2S and HCl concentration limits in the fuel for anode supported SOFC operation. *Cent Eur J Chem*. 2013;11:960-967.
54. Bao JE, Krishnan GN, Jayaweera P, Perez-Mariano J, Sanjurjo A. Effect of various coal contaminants on the performance of solid oxide fuel cells: part I. Accelerated testing. *J Power Sources*. 2009;193:607-616.
55. Reeping KW, Kirtley JD, Bohn JM, Steinhurst DA, Owrutsky JC, Walker RA. Chlorine-induced degradation in solid oxide fuel cells identified by operando optical methods. *J Phys Chem C*. 2017;121:2588-2596.
56. Madi H, Lanzini A, Papurello D, et al. Solid oxide fuel cell anode degradation by the effect of hydrogen chloride in stack and single cell environments. *J Power Sources*. 2016;326:349-356.
57. Pumiglia D, Vaccaro S, Masi A, et al. Aggravated test of intermediate temperature solid oxide fuel cells fed with tar-contaminated syngas. *J Power Sources*. 2017;340:150-159.
58. Cavalli A, Kunze M, Aravind PV. Cross-influence of toluene as tar model compound and HCl on solid oxide fuel cell anodes in integrated biomass gasifier SOFC systems. *Appl Energy*. 2018;231:1-11.
59. Sharma M, Rakesh N, Dasappa S. Solid oxide fuel cell operating with biomass derived producer gas: status and challenges. *Renew Sustain Energy Rev*. 2016;60:450-463.
60. Ud Din Z, Zainal ZA. The fate of SOFC anodes under biomass producer gas contaminants. *Renew Sustain Energy Rev*. 2017;72:1050-1066.
61. Brunner T, Ramerstorfer C, Obernberger I, et al. Development of a highly efficient micro-scale CHP system based on fuel-flexible gasification and a SOFC. 25th Eur. Biomass Conf. Exhib., 2017, p. 725-731.
62. Thermfact/CRCT, GTT-Technologies. FactSage n.d. www.factsage.com
63. Hagen A, Johnson GB, Hjalmarsson P. Electrochemical evaluation of sulfur poisoning in a methane-fuelled solid oxide fuel cell: effect of current density and sulfur concentration. *J Power Sources*. 2014;272:776-785.
64. He HP, Wood A, Steedman D, Tilleman M. Sulphur tolerant shift reaction catalysts for nickel-based SOFC anode. *Solid State Ionics*. 2008;179:1478-1482.
65. Kromp A, Dierickx S, Leonide A, Weber A, Ivers-Tiffée E. Electrochemical analysis of sulphur-poisoning in anode-supported SOFCs under reformate operation. *ECS Trans*. 2012;41:161-169.

66. Basagiannis AC, Verykios XE. Reforming reactions of acetic acid on nickel catalysts over a wide temperature range. *Appl Catal A Gen*. 2006;308:182-193.
67. Kuhn JN, Lakshminarayanan N, Ozkan US. Effect of hydrogen sulfide on the catalytic activity of Ni-YSZ cermets. *J Mol Catal A Chem*. 2008;282:9-21.
68. Richardson JT, Ortego JD, Coute N, Twigg MV. Chloride poisoning of water-gas shift activity in nickel catalysts during steam reforming. *Catal Letters*. 1996;41:17-20.

How to cite this article: Cavalli A, Bernardini R, Del Carlo T, Aravind PV. Effect of H_2S and HCl on solid oxide fuel cells fed with simulated biosyngas containing primary tar. *Energy Sci Eng*. 2019;7:2456–2468. https://doi.org/10.1002/ese3.434